Bottomhole Pressure Inversion Method for Open-Circuit Drilling Based on Drilling Fluid Return Height

Gang Chen[1], Zhengfeng Shan[2], Xiansi Wang[1,2], Jie Zhong[1,3], and Zhiyuan Wang[1,3(✉)]

[1] School of Petroleum Engineering, China University of Petroleum (East China), Qingdao 266580, China
wangzy1209@126.com
[2] CNPC Offshore Engineering Co., Ltd., Tianjin 300451, China
[3] National Engineering Research Center of Oil and Gas Drilling and Completion Technology, Qingdao, Shandong, People's Republic of China

Abstract. In the process of shallow deepwater drilling, due to the narrow safety window of drilling fluid density and the frequent drilling in shallow gas, shallow flow, gas hydrate and other factors, the risk of drilling accidents increases, and kick and even blowouts are easy to occur, which seriously endangers the safety of operators. In the absence of risers and subsea blowout preventers, open-circuit drilling is usually used to drill deep water shallow drilling. In the process of open-circuit drilling, drilling fluid directly returns to the seabed, so it is impossible to shut in the well when kick or even blowout occurs, and it is difficult to obtain the shut-in vertical pressure and casing pressure through traditional methods, and it is difficult to calculate the bottomhole pressure, which cannot provide a basis for the selection of parameters such as density and displacement of subsequent kill fluid. Aiming at this problem, based on Fluent numerical simulation software, this paper simulated and studied the return form of drilling fluid at the bottom mud line of open-circuit drilling by solving the VOF model, and analyzed the influence of different ocean current velocity distribution, drilling fluid displacement, gas penetration on the return height of drilling fluid. It is found that ocean current velocity distribution has little influence on drilling fluid return height, and mainly affects the diffusion dilution degree of drilling fluid. Drilling fluid displacement, gas penetration and wellhead pressure have great influence on drilling fluid return displacement and height. On this basis, according to the principle of underwater jet, the relationship between drilling fluid return height and wellhead pressure is established. On the premise of known return height, the wellhead pressure can be calculated, and the bottomhole pressure can be retrieved from the wellhead pressure. This study reveals the regularities of drilling fluid return flow in open-circuit drilling, provides theoretical guidance for the prediction of bottomhole pressure when kick occurs and the well cannot be shut in, provides support for the effective implementation of subsequent well control measures, and ensures the operation safety of deep-water shallow open-circuit drilling.

Keywords: open-circuit drilling · drilling fluid return · bottomhole pressure inversion · deep water drilling · Fluent numerical simulation

B. Sun et al. (Eds.): DWOG-Hyd 2023, LNCE 472, pp. 40–52, 2024.
https://doi.org/10.1007/978-981-97-1309-7_4

1 Introduction

Deepwater oil and gas resources are the main global energy replacement field in the 21st century. In addition, the South China Sea region has rich oil and gas resources, 70% of which are located in deepwater areas. The exploration and development of deepwater oil and gas fields are of great significance to the national economic development and energy security.

The exploration and development process of deepwater oil and gas fields is complex and faces many uncertain factors. If not properly handled, it will lead to major safety accidents, resulting in property and life losses and damage to the natural environment. Deepwater drilling adopts different drilling methods according to different layers and different construction requirements. In the process of deepwater shallow drilling, due to the shallow layer and unstable stratum structure, in order to save drilling costs and shorten drilling time, open-circuit drilling is generally used to make the drilling fluid directly return to the seabed. However, the shallow geological disasters such as shallow gas, shallow flow and natural gas hydrate are often accompanied by the shallow geological disasters in the shallow layer of deepwater shallow layer. In addition, the density window of deepwater safe operation is narrow, so it is easy to occur well blowout or even blowout. In view of the problems existing in deepwater shallow open-circuit drilling, the drilling fluid return law during well blowout is studied. According to the drilling fluid return height, the wellhead pressure is calculated and the bottomhole pressure is inverted. It can provide effective well information for technicians at the early stage of well blowout and provide technical support for the implementation of subsequent well control measures.

In the process of open-hole deepwater drilling, the process of drilling fluid returning at the mudline of the seabed is a jet phenomenon. Because of the density difference between the returning drilling fluid and the surrounding seawater, the returning drilling fluid is affected by both the initial momentum and the buoyancy, and the returning process of drilling fluid is a buoyancy jet. According to the direction of the buoyancy jet, the buoyancy jet is divided into positive buoyancy jet and negative buoyancy jet [1]. When the direction of the buoyancy is the same as the direction of the initial momentum, it is a positive buoyancy jet, and vice versa, it is a negative buoyancy jet [2]. Because the density of the returning drilling fluid is greater than that of the seawater, the returning process of drilling fluid is a negative buoyancy jet. As an important branch of buoyancy jet, negative buoyancy jet has become a very important topic in the field of hydrodynamics in recent years, and has been paid more and more attention. Hua Zhang et al. [3] conducted a detailed experimental study on the maximum rising height of vertical jet in a static environment. Turner [5], Philip J.W. Roberts et al. [4] conducted experiments on circular inclined jets in static and flowing environments, and obtained the corresponding formulas for the maximum rising height of the jet, the position of the impact point and the dilution. For the numerical simulation research in the cross flow environment, Qi Meilan et al. [6] and Deamaren et al. [7] conducted numerical simulations on the circular hole jet, and presented the contour maps and distribution curves of flow velocity and concentration. Later, Wei Li et al. [8] established a mathematical model that can systematically simulate and accurately predict this kind of flow, and obtained the distribution of physical quantities on the jet symmetric plane, the relationship between the jet core and the flow velocity ratio, etc. It is difficult to obtain the internal structure of the flow field

by means of realistic experiments. The numerical simulation method can obtain more comprehensive flow field structure data, and improve the research level of this type of jet.

2 Fluent Numerical Simulation

2.1 Fundamental Governing Equation

(1) Mass conservation equation

The equation of conservation of mass, also called the equation of continuity, states that the added mass in a microelement per unit time is equal to the net mass flowing into the microelement during the same period. Any problem of fluid flow should be governed by the law of conservation of mass.

$$\frac{\partial \rho}{\partial t} + \nabla \cdot (\rho \vec{v}) = S_m \tag{1}$$

where, ρ is fluid density, kg/m^3; t is time, s; $\vec{v}$ is the velocity vector, m/s; S_m is the source term, representing the mass added to the continuous phase, or it can be any other custom source term.

(2) Momentum conservation equation

The conservation of momentum equation states that the sum of the external forces acting on a microelement in unit time is equal to the rate of change of momentum in the microelement with respect to time. It is the law of conservation of momentum that any flow problem needs to follow.

$$\frac{\partial}{\partial t}(\rho \vec{v}) + \nabla \cdot (\rho \vec{v}\vec{v}) = -\nabla p + \nabla \cdot \left[\mu\left(\nabla \vec{v} + \vec{v}^T\right)\right] + \rho \vec{g} + \vec{F} \tag{2}$$

where, P is pressure, Pa; $\vec{F}$ is the unit mass force, m/s^2; μ is the dynamic viscosity, N·s/m^2; $\vec{g}$ is the acceleration of gravity, m/s^2.

2.2 Geometric Model and Meshing

(1) Geometric model

In this paper, the Fluent numerical simulation is conducted for drilling fluid backflow in the process of shallow open-circuit drilling in deep water. Therefore, the geometric model is established based on the key Eulerian domain distribution of drilling fluid backflow, as shown in Fig. 1. The drill pipe and annulus sizes of the model are set according to the real sizes of a drilling in the South China Sea (Table 1).

(2) Meshing

Poly-hexcore grid is adopted for simulation grid division in this paper. Poly-hexcore grid is mainly composed of hexahedral units, which has good accuracy and precision and is highly adaptable. It can realize automatic region encryption, ensure calculation accuracy and save more calculation time, as shown in Fig. 2.

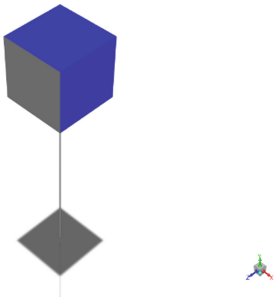

Fig. 1. Geometric model

Table 1. Geometric parameters of the model

Ocean depth(m)	Wellbore diameter(m)	Drill pipe diameter(m)	Wellbore depth(m)
10	0.51	0.14	30

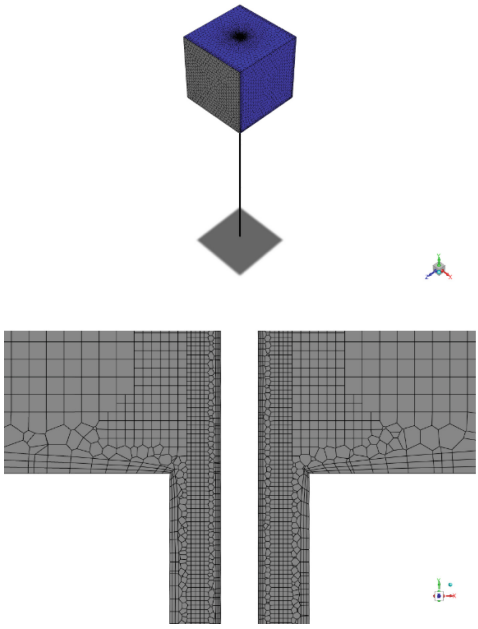

Fig. 2. Model meshing

2.3 Flow Model and Boundary Conditions

(1) Multiphase flow model

This paper uses the VOF model in Fluent software, which is a method for dealing with surface tracking based on a fixed Eulerian grid. In this model, only a set of momentum conservation equations is adopted for all fluids. In each calculation unit of the whole flow field, the phase volume ratio of each fluid component is calculated and recorded:

$$\frac{\partial}{\partial t}\left(\alpha_q \rho_q\right) + \nabla \cdot \left(\alpha_q \rho_q \vec{v}_q\right) = S_{\alpha_q} + \sum\nolimits_{p=1}^{n} \left(\dot{m}_{pq} - \dot{m}_{qp}\right) \tag{3}$$

where, α_q is the volume fraction of fluid q and has no dimension; ρ_q is the fluid q density, kg/m^3; $\vec{v}_q$ is the q phase velocity vector, m/s; $\dot{m}_{pq}$ is the mass transfer from fluid p to fluid q; $\dot{m}_{qp}$ is the mass transfer from fluid q to fluid p; S_{α_q} is the source entry.

(2) Turbulence model

Turbulent model chooses the two-equation model standard k-e model in Fluent software, which is proposed according to the experimental research phenomenon. Turbulent kinetic energy equation and turbulent dissipation rate equation are used for solving, and turbulent kinetic energy and dissipation rate can be obtained, and the numerical value obtained is used to calculate turbulent viscosity.

$$\rho \frac{dk}{dt} = \frac{\partial}{\partial x_i}\left[\left(\mu + \frac{\mu}{\sigma_k}\right)\frac{\partial k}{\partial x_i}\right] + G_k + G_b - \rho\varepsilon - Y_m \tag{4}$$

$$\rho \frac{d\varepsilon}{dt} = \frac{\partial}{\partial x_i}\left[\left(\mu + \frac{\mu}{\sigma_\varepsilon}\right)\frac{\partial \varepsilon}{\partial x_i}\right] + C_{1s}\frac{\varepsilon}{k}(G_k + C_{3s}G_b) - C_{2s}\rho\frac{\varepsilon^2}{k} \tag{5}$$

where, ρ is fluid density, kg/m^3; x_i is position; μ is fluid viscosity, pa·s; G_k is turbulent energy generation caused by average velocity gradient; G_b is turbulent energy generation caused by buoyancy; Y_m is the effect of compressible turbulent pulsation on total dissipation rate; C_{1s}, C_{2s}, C_{3s} are set as default values in Fluent software, respectively 1.44, 1.92, 0.99; k is turbulent energy; ε is dissipation rate.

(3) Boundary conditions

Set boundary conditions such as velocity inlet, pressure outlet and wall. In order to simulate the real seabed environment to the maximum extent, seawater velocity adopts logarithmic velocity profile, and the ocean current velocity flow distribution formula is:

$$\mathrm{V} = V_{max}\left[\frac{2y}{H} - \left(\frac{y}{H}\right)^2\right] \tag{6}$$

where, V_{max} is the maximum ocean current velocity on free surface, which is taken as 0.3–0.5 m/s in this paper; H is the depth of seabed wellhead; y is the height variable (0 $\leq$ y $\leq$ H).

Except for the inlet and outlet, the rest boundaries are set as wall, so the mechanical properties of seabed, including deformation caused by force, are ignored.

2.4 Simulation Results and Verification

(1) Simulation results

The simulation results of different ocean current velocities are as follows (Figs. 3, 4 and 5):

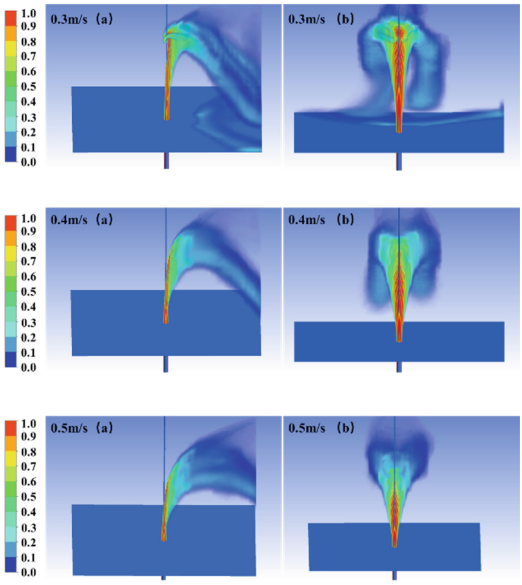

Fig. 3. Drilling fluid return under different ocean current velocities

The simulation results of different drilling fluid displacement are as follows:
The simulation results of drilling fluid return with different gas influx are as follows:

(2) Verification

By comparing the actual height of drilling fluid return and the simulated height under different gas influx conditions, it is found that the error range between the simulated drilling fluid return height and the actual drilling fluid return height by Fluent is within the allowable range, indicating that the numerical simulation results in this paper are reliable (Figs. 6 and 7).

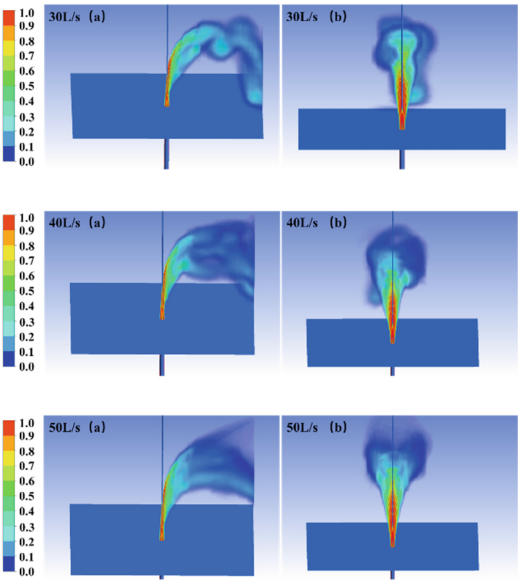

Fig. 4. Drilling fluid return with different drilling fluid displacement

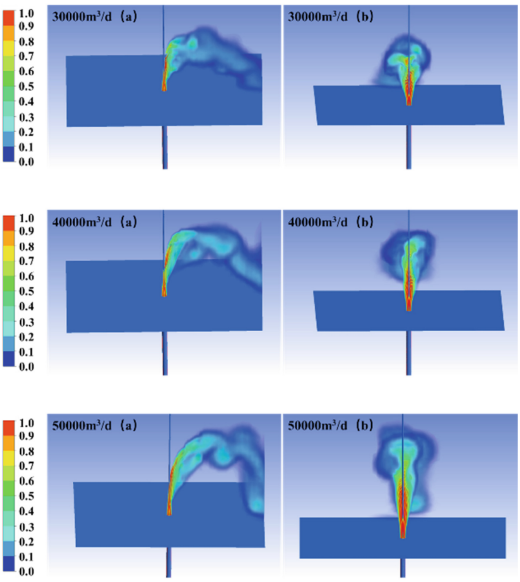

Fig. 5. Drilling fluid return with different gas influx

Fig. 6. Actual height of drilling fluid return and simulated height

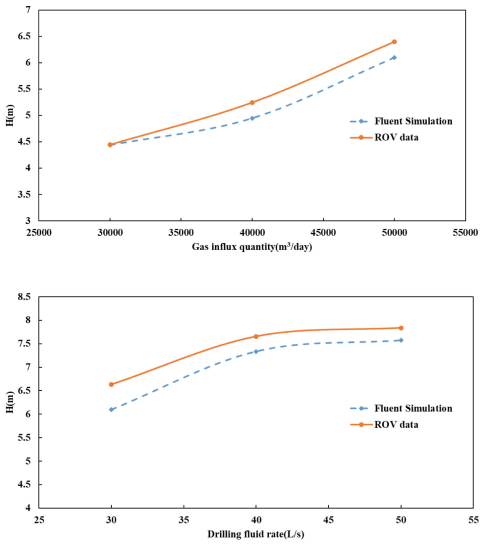

Fig. 7. Comparison of simulation results and ROV data

3 Wellhead Pressure Calculation Based on Drilling Fluid Return Height

According to the jet theory in fluid dynamics, the influence of the resistance at the nozzle on the jet height is ignored, and the single jet theory height is used to represent the drilling fluid return height. Turner [4] concluded through dimensional analysis that the maximum rising height H is related to the momentum flux M, buoyancy flux B and flow flux Q.

$$\mathrm{H} = f(Q, M, B) \tag{7}$$

where, $\mathrm{Q} = \frac{1}{4}\pi d^2 u_0$; $\mathrm{M} = \mathrm{uQ}$; $\mathrm{B} = \frac{1}{4}\pi d^2 u_0 g_0'$; $g_0' = g(\rho_0 - \rho_a)/\rho_a$.

where d is the nozzle diameter, m; u_0 is the flow velocity at the nozzle, m/s; ρ_0 is the jet fluid density, kg/m^3; ρ_0 is the environmental fluid density, kg/m^3; g is the gravitational acceleration, m/s^2.

Thus, two length scales and one flow velocity scale are obtained:

$$l_M = M^{3/4}B^{-1/2} \quad 、 \quad l_Q = QM^{-1/2} \quad 和 \quad u_c = B^{1/2}M^{1/4} \tag{8}$$

(8)

where, l_M is the momentum characteristic length; l_Q is the flow characteristic length. Based on the three characteristic lengths, Eq. (7) can be written as:

$$H = f(Q, B, M, u_a, \theta, \varphi) \tag{9}$$

where,is the flow velocity of environmental fluid, m/s;is the angle between the nozzle normal direction and the bottom surface;is the angle between the flow velocity of environmental fluid and the vertical plane through the nozzle.In this paper, the drilling fluid return process of open-circuit drilling is vertical jet, so Eq. (9) is:

$$H = f(Q, B, M, u_a) \tag{10}$$

Through dimensional analysis, the length scale and flow velocity scale are introduced, and the above equation is:

$$\frac{H}{l_M} = f\left(\frac{l_M}{l_Q}, \frac{u_a}{u_0}\right) \tag{11}$$

According to the Boussinesq hypothesis, the change of density does not significantly change the properties of fluid, and the density difference before and after mixing is very small compared with the density of each point.Then:

$$g_0' = g\left(\frac{\rho - \rho_a}{\rho_a}\right) = f(Q, M, B, u_a) \tag{12}$$

ρ is the local density of the flow field after mixing, and Eq. (11) is:

$$\frac{u_0^2}{g' l_M} = f\left(\frac{l_M}{l_Q}, \frac{u_a}{u_0}\right) \tag{13}$$

After introducing the Froude number $\mathrm{F} = u_0/\sqrt{g_0' d}$ and the speed ratio $u_r = u_a/u_0$:

$$\frac{H}{dF} = f(F, u_r F) \tag{14}$$

$\frac{l_M}{l_Q}$ is much greater than 1, and the influence of l_Q is ignored:

$$\frac{H}{dF} = f(u_r F) \tag{15}$$

By fitting the numerical simulation results of this paper, the previous empirical formula is modified:

$$\frac{H}{dF} = 2.204(u_r F)^{-1/3} \tag{16}$$

The relationship between the drilling fluid return height H and the wellhead flow velocity u_0 is obtained. Then, the relationship between the wellhead flow velocity and the wellhead pressure is also needed to be established. The relationship between the actual jet flow and the nozzle pressure is:

$$\mathrm{Q} = \sqrt{\frac{BP}{10000}} \tag{17}$$

where, Q is the wellhead flow rate, m^3/s; P is the wellhead pressure, Mpa; B is the flow characteristic coefficient, which is obtained by experiment. The outlet flow rate is converted to the wellhead flow rate, and the relationship between the wellhead flow rate and the wellhead pressure is obtained:

$$u_0 = \frac{4}{\pi d^2}\sqrt{\frac{BP}{10000}} \tag{18}$$

Substitute the above equation into (16), and we get:

$$\mathrm{H} = \frac{2.204(u_r F)^{-1/3}\sqrt{\frac{BP}{g_0' d}}}{25\pi d} \tag{19}$$

The flow characteristic coefficient B in the above equation is only related to the wellhead diameter. The empirical formula obtained by predecessors through experiments is:

$$\mathrm{B} = 22556d^2 - 514.3d + 3.227 \tag{20}$$

Therefore, the relationship between the drilling fluid return height H and wellhead pressure P is established. Under the premise of known drilling fluid return height, the wellhead pressure can be calculated in real time, providing conditions for the inversion of bottomhole pressure.

4 Inversion of Bottomhole Pressure Based on Wellhead Pressure

When overflow occurs, formation gas invades the wellbore, and the single-phase flow in the annulus of the wellbore changes into gas-liquid two-phase flow. Based on the calculation method of wellhead pressure, this paper obtains the gas-liquid two-phase flow state and pressure distribution in the wellbore by solving the gas-liquid two-phase flow model in the wellbore.

4.1 Gas-Liquid Two-Phase Flow Model in the Wellbore During Well Surge

The drift flow model originally proposed by Zuber et al. [9] is selected in this paper. This model describes the relative slip of gas flow and gas-liquid mixed flow, reveals the sliding difference between gas-liquid two-phase flow in two-phase flow and the distribution law of gas-liquid two-phase in the pipeline. The governing equations of the model include

gas phase continuity equation, liquid phase continuity equation and gas-liquid phase mixed momentum equation.

Gas phase continuity equation:

$$\frac{\partial}{\partial t}\left(\rho_g \alpha_g\right) + \frac{\partial}{\partial z}\left(\rho_g \alpha_g u_g\right) = 0 \tag{21}$$

Liquid phase continuity equation:

$$\frac{\partial}{\partial t}\left(\rho_l \alpha_l\right) + \frac{\partial}{\partial z}\left(\rho_l \alpha_l u_l\right) = 0 \tag{22}$$

Mixed momentum equation:

$$\frac{\partial}{\partial t}\left(\rho_l \alpha_l u_l + \rho_g \alpha_g u_g\right) + \frac{\partial}{\partial z}\left(\rho_l \alpha_l u_l^2 + \rho_g \alpha_g u_g^2 + p\right) = -q \tag{23}$$

where, α_l is liquid content; α_g is gas content; ρ_l is liquid phase density, kg/m^3; ρ_g is gas density, kg/m^3; u_l is liquid phase velocity, m/s; u_g is gas phase velocity, m/s; p is pressure, pa; z is space variable, m; q is source term.

In addition to the control equation, four other auxiliary equations are introduced for auxiliary solution:

Gas-liquid two-phase volume fraction relation- ship:

$$\alpha_l + \alpha_g = 1 \tag{24}$$

Gas phase density equation:

$$\rho_g = \frac{p}{a_g^2} \tag{25}$$

Liquid phase density equation:

$$\rho_l = \rho_{l0} + \frac{p - p_0}{a_l^2} \tag{26}$$

The drift velocity relationship proposed by Zuber and Findlay [10]:

$$u_g = C_0 u_m + u_s \tag{27}$$

where, u_s is gas slippage velocity, m/s; C_0 is gas distribution coefficient.

4.2 Solving of Gas-Liquid Two-Phase Flow Model in Wellbore

(1) Discrete format

For time partial derivative, the first-order backward difference is adopted. Taking the gas phase mass conservation equation as an example, the time partial derivative difference format is as follows:

$$\frac{\left(E_g \rho_g\right)^j - \left(E_g \rho_g\right)^{j-1}}{\Delta t} + \frac{\partial\left(E_g \rho_g v_g\right)^j}{\partial x} = 0 \tag{28}$$

Scalar type variables are located in the center of the control unit, and vector type variables are located at the boundary of the control unit.

For the convection terms in the mass conser-vation equation and momentum conser-vation equation, the first-order upwind difference is adopted.Taking the gaseous mass conservation equation as an example, the difference format of the convection term is:

$$\left.\frac{\partial\left(E_g\rho_g v_g\right)}{\partial s}\right|_i = \frac{1}{\Delta x}\left[\left(E_g\rho_g v_g\right)_{i+1/2} - \left(E_g\rho_g v_g\right)_{i-1/2}\right] \tag{29}$$

$$\left(E_g\rho_g v_g\right)_{i+1/2} = \begin{cases} \left(E_g\rho_g v_g\right)_i v_{g,i} > 0 \\ \left(E_g\rho_g v_g\right)_{i+1} v_{g,i} \le 0 \end{cases} \tag{30}$$

The other terms except the convection term are adopted by central difference, for example, the discrete format of the pressure partial differential term in the momentum equation is (Fig. 8):

$$\left.\frac{\partial p}{\partial s}\right|_{i+1/2} = \frac{1}{\Delta x}(p_{i+1} - p_i) \tag{31}$$

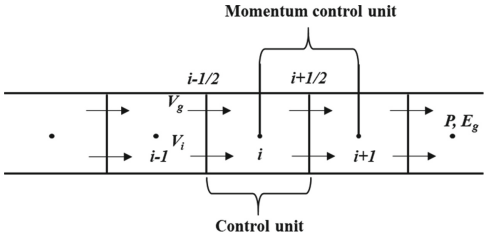

Fig. 8. Schematic diagram of staggered grid difference

(2) Solving steps

①Take the parameters of each node in the wellbore before kick as the initial value, and take the wellhead pressure calculated based on the return height of drilling fluid as the boundary value to estimate the bottomhole pressure.

②Calculate the gas phase density, liquid phase density and other parameters by auxiliary equation.

③Calculate the flux of each node one by one until the wellhead, and compare the calculated results with the actual wellhead pressure. If the accuracy requirements are not met, the bottomhole pressure is re-estimated after correction until the accuracy requirements are met. Thus, the accurate bottomhole pressure is obtained.

5 Conclusion

(1) Through the Fluent simulation of the drilling fluid return process of deepwater shallow open-circuit drilling, the influence of different ocean current velocity on the drilling fluid return height was analyzed, and it was found that the lateral ocean

current velocity had a greater impact on the offset and diffusion of the drilling fluid return, but had a smaller impact on the drilling fluid return height. The influence of different drilling fluid displacement and gas influx on the drilling fluid return height was analyzed, and it was found that the greater the drilling fluid displacement was, the higher the drilling fluid return height was. The greater the drilling fluid displacement was, the higher the drilling fluid return height was, and the change amplitude was more significant than the former.

(2) Based on the relationship between the jet height and the outlet flow velocity, the relationship between the drilling fluid return height and the wellhead flow velocity was obtained by fitting and modifying the Fluent numerical simulation results. The relationship between the drilling fluid return height and the wellhead pressure was further obtained by the relationship between the outlet flow rate and the outlet pressure.

(3) Taking the wellhead pressure as the boundary value, the accurate bottomhole pressure was obtained by solving the drift flow model.Therefore, the bottomhole pressure inversion method for deepwater shallow open-circuit drilling based on the drilling fluid return height was established, which provided a basis for the implementation of subsequent well control measures.

Acknowledgement. The work was supported by the Major Scientific and Technological Innovation Projects in Shandong Province (2022CXGC020407), the CNPC's Major Science and Technology Projects (ZD2019-184-003), the National Natural Science Foundation of China (51991363, 52288101, U21B2069).

References

1. Anderson, J.L., Parker, F.L., Benedict, B.A.: Negatively Buoyant Jets in a Cross Flow. US Government Printing Office (1973)
2. Blevins, R.D.: Applied Fluid Dynamics Handbook. New York (1984)
3. Zhang, H., Baddour, R.E.: Maximum penetration of vertical round dense jets at small and large Froude numbers. J. Hydraul. Eng. **124**(5), 550–553 (1998)
4. Roberts, P.J.W., Toms, G.: Inclined dense jets in flowing current. J. Hydraul. Eng. **113**(3), 323–340 (1987)
5. Turner, J.S.: Jets and plumes with negative or reversing buoyancy. J. Fluid Mech. **26**(4), 779–792 (1966)
6. Mei-lan, Q., Ren-shou, F., Zhi-cong, C.: Computations for plane turbulent impinging jet in cross flow. J. Hydrodyn. Ser. B **11**(4), 23–37 (1999)
7. Demuren, A.O.: Characteristics of three-dimensional turbulent jets in crossflow. Int. J. Eng. Sci. **31**(6), 899–913 (1993)
8. Huai, W., Komatsu, T., Li, W.: Hybrid finite analytic solutions for turbulent jets in cross-flow. In: IAHR, pp. 2060–2069 (1999)
9. Zuber, N., Findlay, J.A.: Average volumetric concentration in two-phase flow systems. J. Heat Transfer **87**(4), 453–468 (1965)
10. Shi, H., Holmes, J.A., Durlofsky, L.J., et al.: Drift-flux modeling of multiphase flow in Wellbores. In: SPE Annual Technical Conference and Exhibition (2003)